

Magnetic relaxation and quantum tunneling of vortices in a polycrystalline $\text{Hg}_{0.8}\text{Tl}_{0.2}\text{Ba}_2\text{Ca}_2\text{Cu}_3\text{O}_{8+\delta}$ superconductor

X. X. Zhang, A. García, and J. Tejada

Departament de Física Fonamental, Facultat de Física, Universitat de Barcelona, Diagonal 647, E-08028 Barcelona, Spain

Y. Xin

Midwest Superconductivity, Inc., Lawrence, Kansas 66049

G. F. Sun and K. W. Wong

Department of Physics and Astronomy, University of Kansas, Lawrence, Kansas 66045

(Received 8 February 1995; revised manuscript received 28 March 1995)

Magnetic relaxation in a polycrystalline $\text{Hg}_{0.8}\text{Tl}_{0.2}\text{Ba}_2\text{Ca}_2\text{Cu}_3\text{O}_{8+\delta}$ [(Hg,Tl)-1223] superconductor was measured in the temperature range 1.85–20 K with different magnetic fields applied during the cooling process. The relaxation curves show a nearly perfect linear $\ln(t)$ behavior. The temperature dependence of the normalized relaxation rate, $R \equiv |d(M/M_0)/d \ln(t)|$, was studied for two applied magnetic fields. With the lower applied field ($H_a = 3$ kOe), a temperature-independent R is found below 2.1 K and explained in terms of quantum tunneling of vortices. As the applied field increases ($H_a = 10$ kOe), the transition from the thermal to the quantum regime is not found in the experimentally accessible temperature range above 1.85 K. The field dependence of R at 2.8 K is studied in order to analyze the dimensionality of the flux-line lattice.

INTRODUCTION

In the last few years, large temperature-independent, time-logarithmic magnetic relaxation at low temperatures in several high- T_c superconductors (HTSC's) has been reported.^{1–10} The temperature dependence of the normalized relaxation rate, $R \equiv |d(M/M_0)/d \ln(t)|$, i.e., the slope of the time-logarithmic curves normalized to the initial magnetization M_0 , was studied. In all those reports, R presents a large, constant value as temperature goes to zero. This effect cannot be accounted for with the models based on thermally activated flux motion,^{11–13} which predict a vanishing magnetic relaxation at zero temperature. Among the suggested mechanisms,^{14,15} quantum tunneling of vortices was proven to be the most plausible explanation for the observed nonthermally activated decay with time. The first description of this phenomenon was given within the quantum creep (QCC) theory by Blatter and co-workers, first for isotropic¹⁶ and later for anisotropic¹⁷ and layered (extremely anisotropic¹⁸) HTSC's. In the framework of the weak collective pinning theory,¹⁹ they derived expressions for the effective Euclidean action of the tunneling process at zero temperature, S_E^{eff} , which is directly related to the normalized relaxation rate as $R \approx \hbar/S_E^{\text{eff}}$.

For anisotropic materials in the single-vortex regime, they obtained, in the limit of strong dissipation,¹⁷

$$R_{\text{QCC,3D}} \approx \hbar/S_E^{\text{eff}} \approx (e^2/\hbar)(\rho_n/L_c). \quad (1)$$

\hbar/e^2 is the quantum of resistance (≈ 4.1 k Ω), ρ_n is the normal-state resistivity in the ab plane extrapolated to zero temperature, and L_c is the collective-pinning length along the c axis, which represents the longitudinal dimen-

sion of the tunneling object:

$$L_c \approx (\xi/\gamma)(j_0/j_c)^{1/2}, \quad (2)$$

where $\gamma \equiv (\lambda_c/\lambda_{ab})$ is the anisotropy parameter (λ_c and λ_{ab} are the London penetration depths along the c axis and the ab plane, respectively), and ξ (superconducting coherence length at zero temperature), j_0 (despairing current density), and j_c (critical current density) denote values in the ab plane.

For discrete layered superconductors, where the collective-pinning length L_c is smaller than the interlayer spacing d , the length of the tunneling object is given by d , so Eq. (1) is replaced by¹⁸

$$R_{\text{QCC,2D}} \approx \hbar/S_E^{\text{eff}} \approx (e^2/\hbar)(\rho_n/d). \quad (3)$$

Very recently, Feigel'man *et al.*²⁰ pointed out that there should be no dissipation in HTSC's at low temperatures. Dissipation of the vortex motion originates from the scattering of the normal excitations, which exist in the bound states at the vortex core.²¹ As temperature decreases, the spacing between the low-lying core levels ω_0 becomes much larger than the level width $1/\tau$. Dissipation is then strongly reduced, and the magnus force becomes the main force in the equation of vortex motion.^{21,22} In this case, Hall tunneling of vortices should be the mechanism responsible for magnetic relaxation at low temperatures. The condition for this limit, $\omega_0\tau \gg 1$, can be expressed as $l \gg \xi(\epsilon_F/\Delta)$, where l is the mean-free path of the normal excitations, ξ is the superconducting coherence length, ϵ_F is the Fermi energy, and Δ is the superconducting gap. This condition is much stronger than the usual condition for the clean limit in type-II super-

conductors, so the material is said to be in the “super-clean” regime. Due to the values of the parameters in the condition [$l \approx 70$ nm, $\xi(\epsilon_F/\Delta) \approx 10\text{--}20$ nm],²⁰ HTSC’s are likely to be in this regime. Feigel’man *et al.*²⁰ obtained the following expressions for the quantum creep rate for HTSC’s in the nondissipative or Hall regime:

$$R_{H,3D} \approx \hbar/S_E^{\text{eff}} \approx (n_s \xi^2 L_c)^{-1}, \quad (4)$$

for an anisotropic material, and

$$R_{H,2D} \approx \hbar/S_E^{\text{eff}} \approx (n_s^{(2)} \xi^2)^{-1}, \quad (5)$$

for a layered superconductor. In these equations, n_s and $n_s^{(2)}$ are the superfluid density in a three-dimensional (3D) system and per superconducting layer, respectively (actually, $n_s^{(2)}$ can be expressed as $n_s t$, where t is the layer thickness), ξ is the superconducting coherence length at zero temperature, and L_c is the longitudinal dimension of the tunneling object.

In this paper we present an observation, by means of magnetic relaxation measurements, of quantum tunneling of vortices in a polycrystalline $\text{Hg}_{0.8}\text{Tl}_{0.2}\text{Ba}_2\text{Ca}_2\text{Cu}_3\text{O}_{8+\delta}$ [(Hg,Tl)-1223] HTSC’s. This material belongs to the recently discovered family of the Hg-based cuprates,²³ and shows the highest zero resistance temperature at atmospheric pressure known to the date.²⁴

EXPERIMENT

The process of preparation of the (Hg,Tl)-1223 superconductor is described in Ref. 24. We just mention here the main steps. A nominal $\text{Ba}_2\text{Ca}_2\text{Cu}_3\text{O}_7$ precursor was first prepared, subsequently mixed with HgO and Tl_2O_3 , and ground in a plastic bag filled with N_2 gas. The cation ratio of $(\text{Hg}_{0.8}\text{Tl}_{0.2})/\text{Ba}/\text{Ca}/\text{Cu}$ was 1223. The ground powder was then pressed into rods of 6 mm in diameter and 15 mm in length. The pressed rods were introduced in a furnace at 860°C for 400 min. After sintering, the sample was annealed in O_2 at 500°C for 10 h. The resistance of the sample was measured by the standard four-probe technique with an ac frequency of 27 Hz. These measurements give a zero resistance temperature $T_c = 138$ K, which is larger than that of Tl-free Hg-1223 phase.²⁴ Powder x-ray diffraction was performed by Cu- $K\alpha$ radiation using a GEIGER-FLEX CN2029 diffractometer. According to the diffraction patterns, the sample is dominated by the 1223 phase, which is greater than 80%. The impurities include the lower T_c phase (Hg,Tl) $\text{Ba}_2\text{CaCu}_2\text{O}_{6+\delta}$ [(Hg,Tl)-1212] and some non-superconducting oxides, such as CaHgO_2 and BaCuO_2 . All the peaks for the 1223 phase in the pattern can be indexed with a tetragonal (space group $P4/mmm$) unit cell, with lattice parameters $a = 3.8574(5)$ Å and $c = 15.794(2)$ Å.²⁴

All magnetic measurements were performed in a commercial (Quantum Design) superconducting quantum interference device magnetometer. The temperature dependence of magnetization was measured as follows. First, the sample was cooled from the normal state down to 5 K, with zero applied magnetic field [zero-field-cooling (ZFC) process]. Then, $H_a = 50$ Oe was applied on and

$M_{\text{ZFC}}(T)$ was measured by heating the sample up to the normal state. Secondly, the sample was cooled with the same applied field, down to 5 K again [field-cooling (FC) process]. Thus, $M_{\text{FC}}(T)$ was measured by heating up the sample. After a ZFC process, initial magnetization curves $M(H)$ with magnetic field applied up to 54 kOe were measured at different temperatures. From these curves, the lower critical field for intergranular (H_{c1}^{inter}) and intragranular (H_{c1}^{gr}) flux penetration, and the first full flux penetration field (H^*), were determined.

The relaxation measurements were performed as follows. The sample was field cooled down from the normal state to the target temperature. In this process, the magnetic field was carefully applied in a no-overshoot mode. The fluctuation of the field in this mode should be less than 0.05 Oe. The sample was then assumed to be homogeneously penetrated. Once the temperature of the sample was stable, the field was removed and the time decay of the remanent magnetization was measured. The evolution of the magnetization is only because of the escape of trapped flux from the sample. At each temperature, the first magnetization point was recorded at 60 s, and subsequent data were taken approximately every 70 s, during a period of 1 h.

RESULTS AND DISCUSSION

Figure 1 presents the ZFC-FC curves obtained with $H_a = 50$ Oe. In this and the following figures, magnetization is expressed in units of emu/g (the mass of sample used in all the measurements was 0.0439 g). The zero-field-cooled diamagnetism at the lowest temperature [$M_{\text{ZFC}}(5\text{ K}) \approx -0.31321$ emu/g] is about 50% of perfect diamagnetic shielding, while the Meissner flux expulsion [$M_{\text{FC}}(5\text{ K}) \approx -0.03736$ emu/g] is small, being approximately a 6% of that of an ideal superconductor. The temperature of onset of the transition from the normal to the superconducting state is defined as the superconducting transition temperature, $T_{c,\text{on}} \approx 133.5$ K. A knee in the data can be observed at $T \approx 110$ K, which could cor-

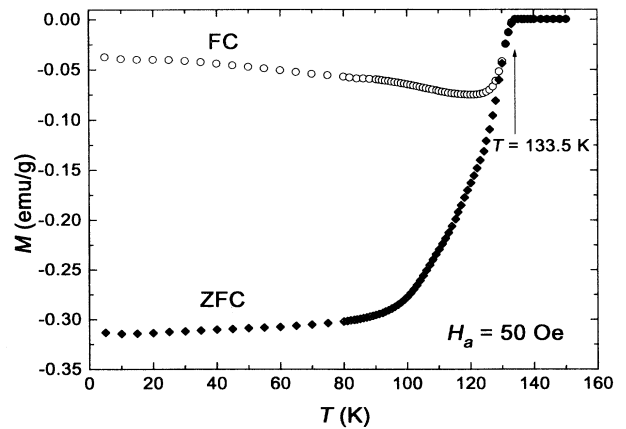


FIG. 1. Temperature dependence of the magnetization $M(T)$ obtained with $H_a = 50$ Oe. The lower and upper curves correspond, respectively, to the ZFC and FC processes (see the text for a description of the processes).

respond to the lower T_c 1212 phase. Initial magnetization curves in the low field range for $T=3$ and 5 K are shown in Fig. 2. The field at which the deviation from the very-low-field linear dependence (Meissner state of the whole sample) occurs, determines the lower critical field for intergranular flux penetration: $H_{c1}^{\text{inter}}(3\text{K}) \approx H_{c1}^{\text{inter}}(5\text{K}) \approx 10 \pm 1$ Oe. As magnetic field increases, a second linear regime corresponding to the Meissner state of grains starts developing at $H_a \approx 35$ Oe. A linear regression allows us to determine the lower critical field for intragranular flux penetration as the field of departure from the linear dependence: $H_{c1}^{\text{gr}}(3\text{K}) \approx 160 \pm 10$ Oe, $H_{c1}^{\text{gr}}(5\text{K}) \approx 140 \pm 10$ Oe. Complete initial magnetization curves with H_a up to 54 kOe are presented in Fig. 3. We chose the peak of each initial $M(H)$ curve as a lower bound for the first full flux penetration field:²⁵ $H^*(3\text{K}) \approx 4.5$ kOe, and $H^*(5\text{K}) \approx 3.8$ kOe. Such a criterion does not affect the analysis of the experimental data here reported.

Figures 4(a) and 4(b) present magnetic relaxation curves obtained at different temperatures (1.85–20 K) with $H_a=3$ kOe applied during the FC process. All curves are linear with the logarithm of time in the scanned time window, except for an initial nonlinear transient decay, which could correspond to a reconfiguration of the inhomogeneous flux distribution, caused by the sudden suppression of the magnetic field just before the measurement started.²⁶ The data were fitted to the logarithmic law $M(t)=a+b \ln(t)$, where $a=M_0=M(t=1\text{s})$, and $b/a=R$. Figure 5 shows the temperature dependence of the normalized relaxation rate $R(T)$. As temperature decreases from 20 K, a maximum at ≈ 8 K is observed, leading to a linear decrease down to $T_p \approx 2.1$ K (see the inset in Fig. 5). Below T_p , R suddenly becomes temperature independent down to 1.85 K. As stated in the Introduction, this temperature independence is the signature of quantum vortex motion. The linear $R(T)$ dependence observed in the thermal re-

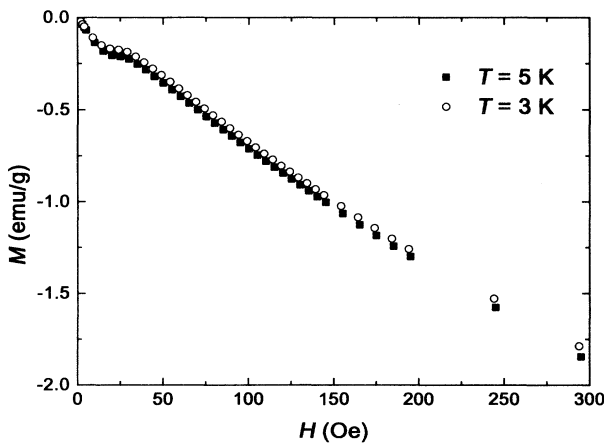


FIG. 2. Low-field dependence of the magnetization $M(H)$ obtained for two different temperatures, $T=3$ and 5 K. The sample was first zero-field-cooled from the normal state down to the target temperature.

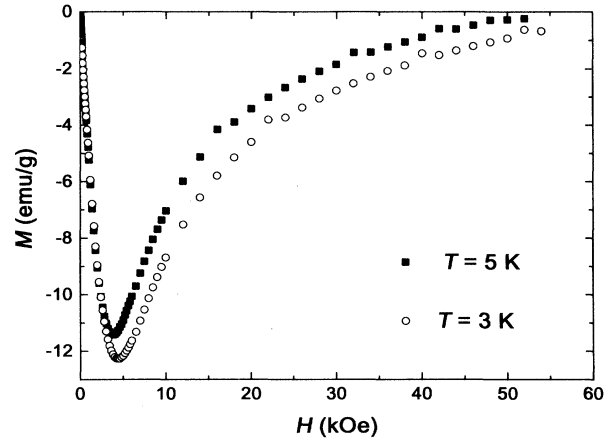


FIG. 3. Initial magnetization curves $M(H)$ in the whole field range (the maximum magnetic field applied was $H_a=54$ kOe). These curves are an extension of the low-field $M(H)$ curves of Fig. 2.

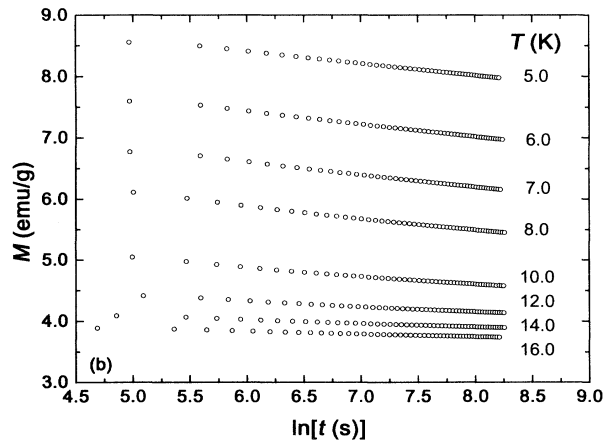
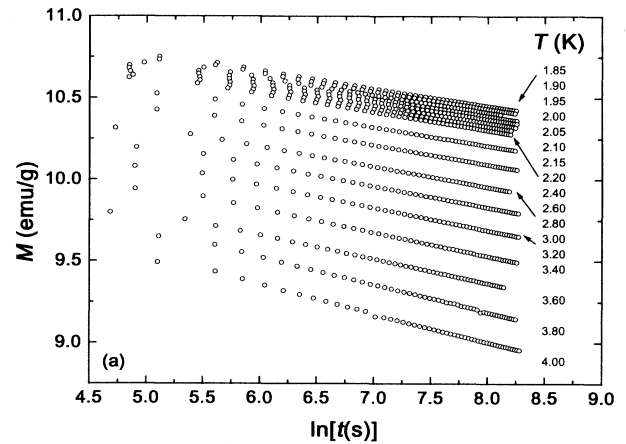


FIG. 4. Magnetic relaxation curves M vs $\ln(t)$ obtained at different temperatures: (a) from 1.85 to 4 K and (b) from 5 to 16 K. The magnetic field applied during the preliminary FC process was $H_a=3$ kOe.

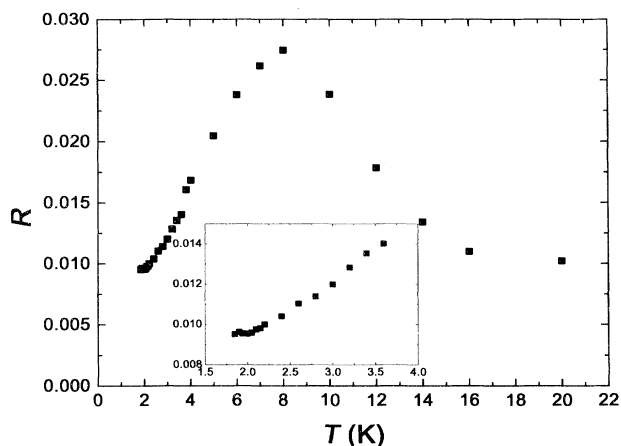


FIG. 5. Temperature dependence of the normalized relaxation rate $R(T)$ obtained with $H_a = 3$ kOe in the FC process. Inset: Magnification of the low-temperature regime (from 1.85 to 3.6 K).

gime is the usual prediction of the simplest model for thermally activated flux motion, the Anderson-Kim model:¹¹ in the investigated low-temperature range, and for the studied time window, $R(T)$ equals $k_B T/U_0$, where U_0 is the average pinning energy, which is temperature independent. In addition, the Bean model²⁷ relates the initial magnetization M_0 , which enters the definition of R , to the critical current density in the absence of thermal activation j_{c0} ($M_0 \propto j_{c0}$). Therefore, the peak in $R(T)$, which is a common feature of many high- T_c superconducting systems,^{26,28} can be explained²⁹ as originating from two competing effects: the explicit linear T dependence and the implicit dropoff with temperature of the critical current density j_{c0} .

A similar $R(T)$ dependence obtained with $H_a = 10$ kOe is shown in Fig. 6. In this case, the maximum occurs at $\simeq 6$ K, and the T -independent regime is not found, indi-

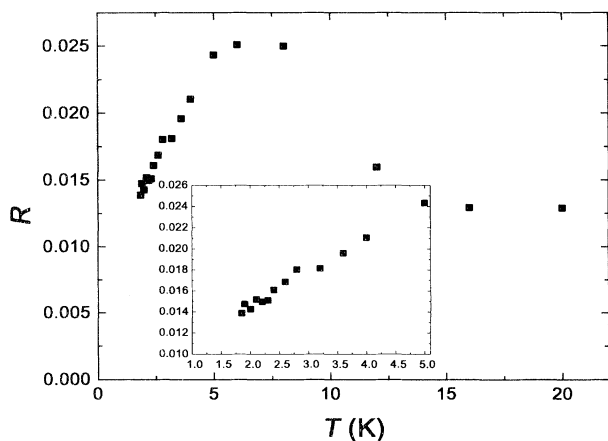


FIG. 6. Normalized relaxation rate as a function of temperature $R(T)$. The inset presents a magnification of the low-temperature regime ($T_{\max} = 5$ K). The field applied during the FC process was $H_a = 10$ kOe.

cating a shifting of the whole curve to temperatures lower than for $H_a = 3$ kOe. This phenomenon can be explained considering that increasing the applied field reduces the energy barrier, which separates two neighboring pinning centers, so thermal activation is still responsible for relaxation at the lowest investigated temperature (1.85 K). Therefore, one should go to temperatures below 1.85 K to find the quantum regime with $H_a = 10$ kOe.

In the following, we will focus our attention on the quantum regime. In order to compare the experimental results with the predictions of the QCC and Hall tunneling theories [Eqs. (1)–(5)], the dimensionality of the flux-line lattice was studied. Figure 7 presents the field dependence of the normalized relaxation rate at $T = 2.8$ K: R increases with H_a up to $\simeq 1$ T and subsequently reaches a saturation value ($\simeq 1.85\%$). This field dependence, which was recently observed by Moehlecke and Kopelevich⁸ in polycrystalline $\text{Bi}_2\text{Sr}_2\text{Ca}_2\text{Cu}_3\text{O}_{10}$, is a manifestation of a crossover in the dimensionality of the flux-line lattice, and it can be explained as follows. HTSC's can be modeled as a stack of weakly Josephson coupled superconducting CuO_2 layers. Application of a magnetic field along the c axis of the system creates 2D pancake vortices within the CuO_2 layers, which interact via Josephson and electromagnetic interaction.³⁰ The actual dimensionality of the flux-line lattice, however, depends on the intensity of the applied magnetic field. Below a dimensional crossover field $H_{3\text{D-2D}} \equiv \Phi_0/(\gamma d)^2$, the Josephson interaction between vortices is important, and the pinning length L_c is larger than the interlayer spacing d . The flux-line lattice is then 3D in nature. Daemen *et al.* recently demonstrated³¹ that in very anisotropic HTSC's, the anisotropy parameter γ increases as H_a increases, directly reflecting the field dependence of the penetration depth along the c axis $\lambda_c(H_a)$. Then, from Eqs. (1), (2), and (4), L_c is expected to decrease and the tunneling rate to increase with the increasing field. Above $H_{3\text{D-2D}}$, L_c becomes smaller than the interlayer spacing d , and the 2D pancake vortices in neighboring layers are essentially

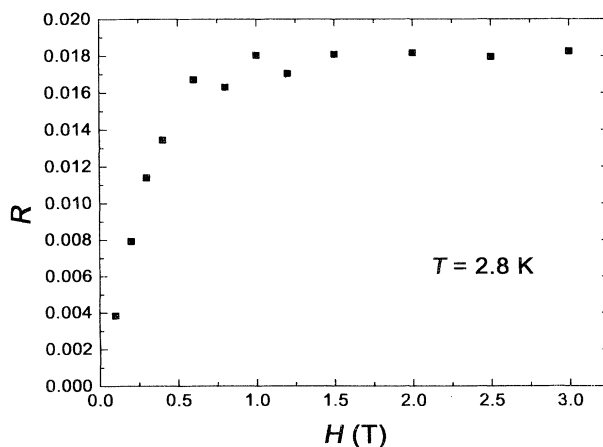


FIG. 7. Field dependence of the normalized relaxation rate $R(H)$ obtained at $T = 2.8$ K. The rates were calculated in the same way as for the $R(T)$ figures.

decoupled. The tunneling rate is then given by Eqs. (3) and (5), in which only field-independent parameters enter the expressions. We would like to remark that the value obtained for the dimensional crossover field, $H_{3D-2D}(2.8 \text{ K}) \simeq 1 \text{ T}$, is just a lower bound for the H_{3D-2D} corresponding to the quantum regime. Nevertheless, as this regime manifests itself up to $T_p \simeq 2.1 \text{ K}$ with $H_a = 3 \text{ kOe}$, $H_{3D-2D}(2.8 \text{ K})$ should be not far from the actual value that one would obtain if the field dependence of R_0 was studied.

From the definition of the dimensional crossover field $H_{3D-2D} = \Phi_0/(\gamma d)^2$, the anisotropy parameter γ can be evaluated. With $H_{3D-2D} \simeq 1 \text{ T}$, and assuming a value for the interlayer spacing d similar to the value of the c axis of the (Hg,Tl)-1223 tetragonal unit cell, $d \sim c \simeq 15.8 \text{ \AA}$, $\gamma \simeq 30$ was obtained. This value, which is similar to the anisotropy parameters of the Tl-2223 ($\gamma \simeq 20$) (Ref. 32) and Bi-2223 ($\gamma \simeq 30$) (Ref. 33) phases, was used to evaluate the theoretical predictions of the QCC and Hall tunneling theories. Using typical numbers for the parameters entering Eqs. (1)–(3) [$\xi_0 \simeq 20 \text{ \AA}$, $(j_0/j_c)^{1/2} \simeq 20$, $\rho_n(0) \simeq 15 \mu\Omega \text{ cm}$], $L_c \simeq d$ and $R_{\text{QCC},3D} \simeq R_{\text{QCC},2D} \simeq 2.3\%$ were obtained. The 2D prediction compares well to the field-independent plateau observed at $T = 2.8 \text{ K}$, $R_{2D}(2.8 \text{ K}) \simeq 1.85\%$. As was argued before, $R_{2D}(2.8 \text{ K})$ is not the tunneling rate, but we expect this value to be similar to the actual 2D quantum creep rate. If we wish to compare the estimations with the experimental plateau observed with $H_a = 3 \text{ kOe}$, we must keep in mind that the applied field is smaller than the dimensional crossover field H_{3D-2D} , so the flux-line lattice should be three dimensional. The value given above for the 3D prediction, $R_{\text{QCC},3D} \simeq 2.3\%$, is larger than $R_0(3 \text{ kOe}) (\simeq 1\%)$ but compares well in order of magnitude. Nevertheless, we believe that $R_{\text{QCC},3D}$ gives an overestimation of the 3D quantum creep rate, because it was evaluated by substituting a constant $L_c (\simeq 10 \text{ \AA})$ in Eq. (1) instead of a field-dependent L_c corresponding to the 3D flux regime [$L_c(H_a)$]. Substitution of a collective-pinning length $L_c(3 \text{ kOe})$ larger than 10 \AA would give a tunneling rate $R_{\text{QCC},3D}(3 \text{ kOe})$ smaller than 2.3% and closer to the experimental value $R_0(3 \text{ kOe}) (\simeq 1\%)$. On the other hand, the Hall tunneling rate can be estimated by substituting in Eqs. (4) and (5) the values for ξ_0 and L_c given above, and considering that in HTSC at low temperatures, n_s is comparable to the carrier density n .²⁰ This gives $R_{\text{H},3D} \simeq R_{\text{H},2D} \simeq 1\%$, which compares fairly well to $R_0(3 \text{ kOe})$. Finally, the crossover temperature from the thermal to the quantum regime T_{qc} may be evaluated by equating the quantum creep and thermal creep rate $R_0 = k_B T_{qc} / U_0$. This gives $T_{qc} \simeq 2.6 \text{ K}$ (with $U_0 \simeq 290 \text{ K}$, as calculated in the thermal regime), in good agreement with the plateau temperature $T_p \simeq 2.1 \text{ K}$.

CONCLUSIONS

The decay with time of the remanent magnetization of a polycrystalline (Hg,Tl)-1223 sample was studied for two magnetic fields applied during the cooling process, $H_a = 3$ and 10 kOe . For both fields, a peak in the temperature dependence of the normalized relaxation rate was observed and explained in terms of thermally activated flux motion. A temperature-independent rate below $T_p \simeq 2.1 \text{ K}$ was found with $H_a = 3 \text{ kOe}$, and interpreted as quantum motion of vortices. This plateau was not detected with $H_a = 10 \text{ kOe}$. The order of magnitude of the plateau was in good agreement with the predictions of the QCC and Hall tunneling theories, but its absolute value compared better to the Hall prediction than to the QCC one. Actually, very recent experiments in 60- and 90-K $\text{YBa}_2\text{Cu}_3\text{O}_{7-\delta}$ demonstrated³⁴ that these materials lie in the superclean regime, so the Hall term should be responsible for the vortex motion at very low temperatures. A similar proof is not available for any other HTSC, not even for (Hg,Tl)-1223. Nevertheless, for lack of actual parameters for (Hg,Tl)-1223 and the uncertainty of the parameters entering the QCC and Hall tunneling estimations, we find it hard to draw a sound conclusion about the mechanism dominating the tunneling process in the present material. Relaxation measurements extending down to very low temperatures (below 1.85 K), together with alternative experiments, need to be performed to go deeply into the knowledge of the mechanisms involved in the quantum tunneling of vortices.

The field dependence of the normalized magnetization rate at $T = 2.8 \text{ K}$ was also studied. The field at which R reached a saturation value was determined as the dimensional crossover field $H_{3D-2D}(2.8 \text{ K}) \simeq 1 \text{ T}$. The saturation value ($\simeq 1.85\%$) compared well to the 2D prediction of the QCC theory ($\simeq 2.3\%$). H_{3D-2D} was used to estimate the anisotropy parameter $\gamma \simeq 30$. This value is larger than the anisotropy parameter given in Ref. 35 for a grain-aligned Tl-free Hg-1223 sample, $\gamma \simeq 7$, obtained by analyzing, with the modified Lawrence-Doniach model,³⁶ normal-state magnetization measurements performed with the magnetic field applied perpendicular to the CuO_2 planes. The incorporation of thallium to the Hg-1223 phase appears to be the most plausible reason for the remarkable increase of the anisotropy parameter.

ACKNOWLEDGMENTS

A.G. thanks the Commissionat per a Universitats i Recerca del Departament de la Presidència de la Generalitat de Catalunya for a research grant. X.X.Z. thanks the Universitat de Barcelona for financial support. J.T. acknowledges financial support from the European Community Project No. ERB4050PL930639.

¹L. Fruchter, A. P. Malozemoff, I. A. Campbell, J. Sanchez, M. Konczykowski, R. Griessen, and F. Holtzberg, Phys. Rev. B **43**, 8709 (1991).

²A. C. Mota, G. Juri, A. Pollini, K. Aupke, T. Teruzzi, and P. Visani, Phys. Scr. **45**, 69 (1992).

³A. García, X. X. Zhang, A. M. Testa, D. Fiorani, and J. Tejada, J. Phys. Condens. Matter **4**, 10341 (1992).

⁴D. Prost, L. Fruchter, I. A. Campbell, N. Motohira, and M. Konczykowski, Phys. Rev. B **47**, 3457 (1993).

⁵S. Uji, H. Aoki, S. Takebayashi, M. Tanaka, and M. Hashimo-

- to, *Physica C* **207**, 112 (1993).
- ⁶J. Tejada, E. M. Chudnovsky, and A. García, *Phys. Rev. B* **47**, 11 552 (1993).
- ⁷K. Aupke, T. Teruzzi, P. Visani, A. Amann, A. C. Mota, and V. N. Zavaritsky, *Physica C* **209**, 255 (1993).
- ⁸S. Moehlecke and Y. Kopelevich, *Physica C* **222**, 149 (1994).
- ⁹A. García, X. X. Zhang, J. Tejada, M. Manzel, and H. Bruchlos, *Phys. Rev. B* **50**, 9439 (1994).
- ¹⁰X. X. Zhang, A. García, J. Tejada, Y. Xin, and K. W. Wong, *Physica C* **232**, 99 (1994).
- ¹¹P. W. Anderson and Y. B. Kim, *Rev. Mod. Phys.* **36**, 39 (1964).
- ¹²M. R. Beasley, R. Labusch, and W. W. Webb, *Phys. Rev.* **161**, 682 (1969).
- ¹³M. V. Feigel'man, V. B. Geshkenbein, and V. M. Vinokur, *Phys. Rev. B* **43**, 6263 (1991).
- ¹⁴E. Simánek, *Phys. Lett. A* **139**, 183 (1989).
- ¹⁵J. Z. Sun, C. B. Eom, B. Lairson, J. C. Bravman, and T. H. Geballe, *Phys. Rev. B* **43**, 3002 (1991).
- ¹⁶G. Blatter, V. B. Geshkenbein, and V. M. Vinokur, *Phys. Rev. Lett.* **66**, 3297 (1991).
- ¹⁷G. Blatter and V. B. Geshkenbein, *Physica C* **185-189**, 2351 (1991).
- ¹⁸G. Blatter and V. B. Geshkenbein, *Phys. Rev. B* **47**, 2725 (1993).
- ¹⁹A. I. Larkin and Yu. N. Ovchinnikov, *Zh. Eksp. Teor. Fiz.* **65**, 1704 (1973) [*Sov. Phys. JETP* **38**, 854 (1973)]; *J. Low Temp. Phys.* **34**, 409 (1979).
- ²⁰M. V. Feigel'man, V. B. Geshkenbein, A. I. Larkin, and S. Levit, *Pis'ma Zh. Eksp. Teor. Fiz.* **57**, 699 (1993) [*JETP Lett.* **57**, 711 (1993)].
- ²¹P. G. de Gennes and J. Matricon, *Rev. Mod. Phys.* **36**, 45 (1964); P. Nozières and F. Vinen, *Philos. Mag.* **14**, 667 (1966).
- ²²N. B. Kopnin and V. E. Kravtsov, *Pis'ma Zh. Eksp. Teor. Fiz.* **23**, 631 (1976) [*JETP Lett.* **23**, 578 (1976)]; *Zh. Eksp. Teor. Fiz.* **71**, 1644 (1976) [*Sov. Phys. JETP* **44**, 861 (1976)].
- ²³S. N. Putilin, E. V. Antipov, O. Chmaissem, and M. Marezio, *Nature (London)* **362**, 226 (1993); A. Schilling, M. Cantoni, J. D. Guo, and H. R. Ott, *ibid.* **363**, 56 (1993).
- ²⁴G. F. Sun, K. W. Wong, B. R. Xu, Y. Xin, and D. F. Lu, *Phys. Lett. A* **192**, 122 (1994).
- ²⁵L. Zhang, J. Z. Liu, R. N. Shelton, and M. D. Lan, *Phys. Rev. B* **50**, 7092 (1994).
- ²⁶C. Rossel and P. Chaudhari, *Physica C* **153-155**, 306 (1988).
- ²⁷C. P. Bean, *Phys. Rev. Lett.* **8**, 250 (1962).
- ²⁸See, for instance, M. Tuominen, A. M. Goldman, and M. L. Mecartney, *Phys. Rev. B* **37**, 548 (1988); *Physica C* **153-155**, 324 (1988); M. E. McHenry, M. P. Maley, E. L. Venturini, and D. L. Ginley, *Phys. Rev. B* **39**, 4784 (1989).
- ²⁹Y. Yeshurun and A. P. Malozemoff, *Phys. Rev. Lett.* **60**, 2202 (1988). An alternative explanation in terms of a distribution of activation energies is given by C. W. Hagen and R. Griessen, *Phys. Rev. Lett.* **62**, 2857 (1989).
- ³⁰J. R. Clem, *Phys. Rev. B* **43**, 7837 (1991).
- ³¹L. L. Daemen, L. N. Bulaevskii, M. P. Maley, and J. Y. Coulter, *Phys. Rev. Lett.* **70**, 1167 (1993); *Phys. Rev. B* **47**, 11 291 (1993).
- ³²O. Laborde, P. Monceau, M. Potel, J. Padiou, P. Gougeon, J. C. Levet, and H. Noel, *Physica C* **162-164**, 1619 (1989).
- ³³I. Matsubara, H. Tanigawa, T. Ogura, H. Yamashita, M. Kinoshita, and T. Kawai, *Phys. Rev. B* **45**, 7414 (1992).
- ³⁴Y. Matsuda, N. P. Ong, Y. F. Yan, J. M. Harris, and J. B. Peterson, *Phys. Rev. B* **49**, 4380 (1994); J. M. Harris, Y. F. Yan, O. K. C. Tsui, Y. Matsuda, and N. P. Ong, *Phys. Rev. Lett.* **73**, 1711 (1994).
- ³⁵M.-K. Bae, M. S. Choi, S. Lee, S.-I. Lee, and W. C. Lee, *Physica C* **231**, 249 (1994).
- ³⁶R. A. Klemm, *Phys. Rev. B* **41**, 2073 (1990).